Mon. Not. R. Astron. Soc. **000**, 000–000 (0000) Printed 13 August 2012 (MN LATEX style file v2.2)

Satellites and Haloes of Dwarf Galaxies

Laura V. Sales[1], Wenting Wang[1,2], Simon D. M. White[1] and Julio F. Navarro[3]

[1] *Max-Planck Institute for Astrophysics, Karl-Schwarzschild-Strasse 1, 85740 Garching, Germany*
[2] *Key Laboratory for Research in Galaxies and Cosmology of Chinese Academy of Sciences, Max-Planck-Institute Partner Group, Shanghai Astronomical Observatory, Nandan Road 80, Shanghai 200030, China*
[3] *Department of Physics and Astronomy, University of Victoria, Victoria, BC, V8P 5C2, Canada*

13 August 2012

ABSTRACT

We study the abundance of satellite galaxies as a function of primary stellar mass using the SDSS/DR7 spectroscopic catalogue. In contrast with previous studies, which focussed mainly on bright primaries, our central galaxies span a wide range of stellar mass, $10^{7.5} \leqslant M_*^{\rm pri}/M_\odot \leqslant 10^{11}$, from dwarfs to central cluster galaxies. Our analysis confirms that the average number of satellites around bright primaries, when expressed in terms of satellite-to-primary stellar mass ratio ($m_*^{\rm sat}/M_*^{\rm pri}$), is a strong function of $M_*^{\rm pri}$. On the other hand, satellite abundance is largely independent of primary mass for dwarf primaries ($M_*^{\rm pri} < 10^{10}\,M_\odot$). These results are consistent with galaxy formation models in the ΛCDM scenario. We find excellent agreement between SDSS data and semi-analytic mock galaxy catalogues constructed from the Millennium-II Simulation. Satellite galaxies trace dark matter substructure in ΛCDM, so satellite abundance reflects the dependence on halo mass, M_{200}, of both substructure and galaxy stellar mass (M_*). Since dark matter substructure is almost scale-free, the dependence of satellite abundance on primary mass results solely from the well-defined characteristic mass in the galaxy mass-halo mass relation. On dwarf galaxy scales, where models predict a power-law scaling, $M_* \propto M_{200}^{2.5}$, similarity is preserved and satellite abundance is independent of primary mass. For primaries brighter than the characteristic mass of the M_*-M_{200} relation, satellite abundance increases strongly with primary mass. Our results provide strong support for the steep, approximately power-law dependence of dwarf galaxy mass on halo mass envisioned in ΛCDM galaxy formation models.

Key words: Galaxies: dwarf – Galaxies: formation – Galaxies: haloes

1 INTRODUCTION

Matching the galaxy luminosity function in the ΛCDM scenario requires that the stellar mass of galaxies, M_*, should vary strongly with the virial[1] mass, M_{200}, of their surrounding dark matter haloes. This exercise implies that the "efficiency" of galaxy formation, as measured by the ratio M_*/M_{200}, decreases steadily toward both smaller and larger masses from a maximum at $M_{200} \sim 10^{12} M_\odot$ (Moster et al. 2010; Behroozi et al. 2010; Guo et al. 2010, 2011a). On the scale of dwarf galaxies ($M_* < 10^{10}\,M_\odot$) these models require a near power-law dependence, $M_* \propto M_{200}^{2.5}$, in order to reproduce observations of faint objects. Such a steep M_*-M_{200} relation implies that dwarfs differing by as much as three decades in stellar mass (e.g., from the Fornax dwarf spheroidal to the Large Magellanic Cloud) inhabit haloes spanning just over one decade in virial mass. Furthermore, very few galaxies exceeding $10^6\,M_\odot$ are expected to have haloes with virial masses below $10^{10}\,M_\odot$.

These predictions have been recently challenged by a series of observations, including (i) the lack of a characteristic velocity at the faint-mass end of blind HI surveys (expected if most dwarfs live in similar haloes, Zwaan et al. 2010; Papastergis et al. 2011); and (ii) the low virial mass (substantially below $10^{10}\,M_\odot$) inferred from dynamical data for the dwarf spheroidal companions of the Milky Way (Boylan-Kolchin et al. 2012) and for nearby dwarf irregulars (Ferrero et al. 2011). The evidence, however, is indirect, since halo masses are estimated by extrapolating data that probe only the inner few kiloparsecs, where most baryons reside.

We explore here the possibility of using satellite galaxies to help constrain the virial masses of dwarf galaxies. The orbital motions of satellite companions have often been used to estimate halo masses (see, e.g., Zaritsky et al. 1997; Erickson et al. 1999; McKay et al. 2002; Prada et al. 2003; van den Bosch et al. 2004;

[1] Virial quantities are defined at the radius from the center of each halo where the mean enclosed density equals 200 times the critical density of the Universe and are identified by a 200 subscript. Units assume a Hubble constant of $H_0 = 73$ km s^{-1} Mpc^{-1} unless otherwise specified.

Brainerd 2005; Conroy et al. 2007), but this work has largely been restricted to systems similar to or brighter than the Milky Way. This is partly due to the difficulties in obtaining redshifts for faint objects. In addition, satellite companions are less common around dwarf galaxies than around larger systems: the number of satellites brighter than a certain fraction of the primary luminosity, $N(> L^{\rm sat}/L^{\rm pri})$, declines strongly toward fainter primaries (e.g. Guo et al. 2011b; Wang & White 2012). Dwarf galaxy associations do exist, but only a handful have been observed (e.g., Tully et al. 2006).

In ΛCDM, where satellite galaxies are thought to trace the substructure of cold dark matter haloes, satellite systems are expected around all central galaxies, regardless of luminosity. The number of satellites, and their dependence on primary mass, should just reflect the abundance of substructure modulated by the dependence of galaxy formation efficiency on halo mass.

Substructure abundance has been studied extensively through numerical simulations, and shown to be nearly invariant with halo mass (Moore et al. 1999; Kravtsov et al. 2004; Gao et al. 2004; Wang et al. 2012). This result, together with the strict constraints on galaxy formation efficiency mentioned above, imply that satellite number counts provide useful information on the halo mass of dwarf galaxies. In particular, the near self-similarity of cold dark matter haloes provides an instructive test: if satellite galaxies trace substructure then the abundance of *luminous* satellites should also be scale-free on scales where galaxy mass and halo mass are related by a featureless power-law.

We explore these issues here by identifying primary-satellite systems in galaxy catalogues constructed from the Sloan Digital Sky Survey and by comparing them with predictions from a semi-analytic mock galaxy catalogue based on the Millennium Simulations. The plan for this paper is as follows. Sec. 2 describes briefly the observational and model datasets while Sec. 3 presents our main results. We summarize our main conclusions in Sec. 4.

2 DATA AND CATALOGUES

2.1 Satellite and primary galaxies in SDSS/DR7

We select primary galaxies spanning a wide range of stellar mass, $7.5 \leqslant \log(\mathrm{M}_*/\mathrm{M}_\odot) \leqslant 11$, from the spectroscopic New York University Value Added Galaxy Catalog (NYU-VAGC). This catalogue was built on the basis of the seventh data release of the Sloan Digital Sky Survey (SDSS/DR7; Blanton et al. 2005; Abazajian et al. 2009).

We ensure isolation by imposing two conditions: (i) each primary must be the brightest of all objects projected within its virial radius with line-of-sight velocities differing by less than three times the corresponding virial velocity; and (ii) no primary can be located within the virial radius of a more massive system. Virial quantities are inferred from the stellar mass, assuming the abundance-matching M_*-M_{200} relation of Guo et al. (2010). Fainter galaxies within a projected distance $r_p < r_{200}$ and a line-of-sight velocity difference $|\Delta V_{\rm l.o.s}| < 3V_{200}$ are then classified as satellites (see Sec. 2.2). We have checked that our results are not sensitive to variations by factors of a few in these thresholds, nor to the addition of 0.2-0.35 dex scatter to the M_*-M_{200} relation.

We apply volume and edge corrections to our sample in the same way as Wang & White (2012). Completeness for SDSS spectroscopic data is estimated to be $\sim 90\%$ for apparent r-band magnitudes brighter than $m_r = 17.7$ (Blanton et al. 2005). This means

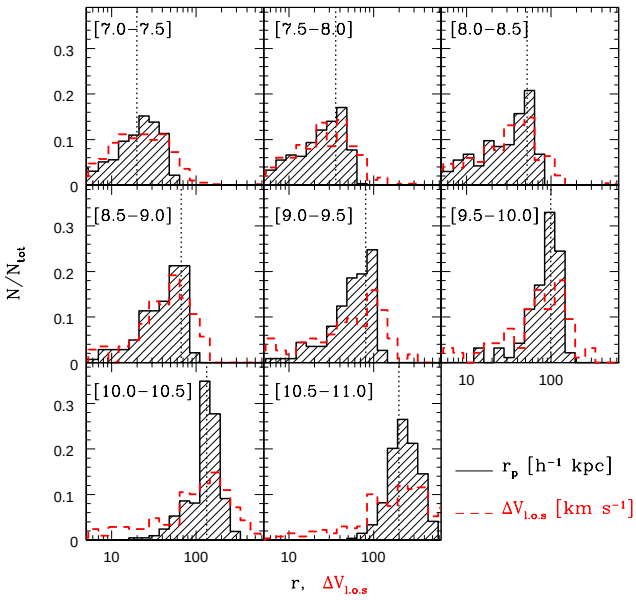

Figure 1. Distributions of projected distance (black) and line-of-sight velocity difference (red) for satellite galaxies in the semianalytic catalogue, binned by primary stellar mass. The minimum and maximum mass of each bin is quoted in each panel (in units of $\log(M_*^{\rm pri}/M_\odot)$). The distributions peak at around the virial radius and velocity corresponding to each bin (vertical dotted line).

that the effective volume where satellites of a given absolute magnitud difference with the primary, $\Delta M = M_r^{\rm sat} - M_r^{\rm pri}$, are (almost) complete varies strongly with $M_r^{\rm pri}$, or equivalently, with primary mass. For instance, the average distance of primary galaxies with $10.3 < \log(M_*/M_\odot) < 11$ is 320 Mpc when counting satellites about a magnitude fainter. This number halves for primaries with $M_* \sim 10^{10} M_\odot$, and drops to 35 Mpc for centrals with $7.5 < \log(M_*/M_\odot) < 8$. Despite the smaller volume surveyed for low mass galaxies, there are enough galaxies to probe the satellite population of even the faintest primaries in our sample.

One might think that the detection of faint objects would be aided by selecting satellites from the photometric catalogue; which is complete down to ~ 4 magnitudes fainter than the spectroscopic sample. This requires the stacking of primary galaxies and a statistical background subtraction in order to identify the excess count corresponding to satellites (Lorrimer et al. 1994; Lares et al. 2011; Nierenberg et al. 2011; Guo et al. 2011b; Wang & White 2012). However, the signal-to-noise to carry out this subtraction is too low for our faint primaries ($M_*^{\rm pri} < 10^9 M_\odot$). Our sample is then selected purely from the spectroscopic catalogue. We discuss briefly possible biases affecting faint, low surface brightness companions in Sec 3.

2.2 Satellite and primary galaxies in the semi-analytic model

We compare our SDSS results with the semi-analytic catalogue of Guo et al. (2011a), based on the dark matter only Millennium-II Simulation (hereafter MS-II, Boylan-Kolchin et al. 2011). The model parameters are carefully tuned to reproduce the observed abundance of low-redshift galaxies over five orders of magnitude in stellar mass and 9 mag in luminosity. The semi-analytic data

contain full 3D velocity and positional information for all galaxies, and thus enables the evaluation of potential biases that may be induced by the limited (projected) data available in observational surveys.

Fig. 1 and 9 of Guo et al. (2011a) shows that predictions for galaxy mass are reliable in simulated haloes resolved with at least $\sim$ 200-300 dark matter particles. This corresponds roughly to $M_{200} \sim 2 \times 10^9 M_\odot$ and $M_* \sim 10^6 M_\odot$ in MS-II. We therefore consider only galaxies with $M_* \geqslant 10^6 M_\odot$ in the analysis below.

Galaxies in the semi-analytic catalogue inhabit dark matter haloes and subhaloes identified using the SUBFIND group-finder algorithm (Springel et al. 2001). Primary galaxies are the central objects of each halo; all other galaxies within the virial radius are considered satellites. The catalogue also includes "orphan" galaxies whose subhaloes have been disrupted due to numerical resolution effects. The catalogue contains more than $157,000$ primary galaxies in the mass range $7 \leqslant \log(\mathrm{M_*/M_\odot}) \leqslant 12$.

The semi-analytic data can be "projected" to mimic the same satellite identification algorithm used for SDSS data (see, e.g., Wang & White 2012 for details). Notice that, because of the different identification criteria applied, the projected satellite and primary samples selected from the mock catalogue differ from the 3D samples (where we use information about the condition as central/satellite object from the SUBFIND catalogues). This enables us to calibrate the parameters of the identification procedure in order to minimize the contribution of foreground and background objects in our primary/satellite sample.

Fig 1 show the distributions of projected distance (r_p, shown in black) and line-of-sight velocity difference ($\Delta V_{\rm l.o.s}$, shown in red) between primaries and "true" satellites, grouped in several bins of primary stellar mass. All histograms peak at the mean virial radius and virial velocity of host haloes in each subsample, indicated by the vertical dotted line. Although, by definition, satellites must be within the virial radius (i.e. $r_p < r_p^{\rm max} = r_{200}$), the upper bound of the velocity difference is less clear, as the escape velocity typically exceeds the virial velocity of a halo substantially in the inner regions. The red histograms in Fig. 1 suggest that the large majority of true satellites have line-of-sight velocities that differ from their primaries by less than $\sim 3V_{200}$. These considerations justify the choices $r_p^{\rm max} = r_{200}$ and $\Delta V_{\rm l.o.s}^{\rm max} = 3\,V_{200}$ made to identify satellite/primary systems in the observational sample (Sec. 2.1).

3 RESULTS

As discussed in Sec. 1, the galaxy-halo mass relation is expected to leave a clear imprint on the abundance of satellites galaxies as a function of primary stellar mass. We explore these ideas in Fig. 2 using the semi-analytic catalogue described in Sec. 2.2.

Fig. 2 shows, as a function of satellite-to-primary mass ratio, the average number of satellites orbiting primaries of different mass in the semi-analytic galaxy catalogue. Primaries are binned in logarithmic M_* bins of 0.5 dex width; the central mass value is quoted in the legend. Satellites are identified in 3D, using the full position and velocity information available in the catalogue.

Fig. 2 shows clearly that the average number of satellites of bright primaries increases strongly with $M_*^{\rm pri}$. On average, a primary as massive as $10^{11.5} M_\odot$ is surrounded by roughly 10 satellites more massive than $0.1\,M_*^{\rm pri}$. On the other hand, only $\sim 40\%$ of primaries as massive as the Milky Way ($10^{10.75} M_\odot$) have one satellite proportionally as massive. The probability of having a companion with $m_*^{\rm sat}/M_*^{\rm pri} = 0.1$ drops further to $\sim 10\%$ for $M_*^{\rm pri} = 10^{10} M_\odot$.

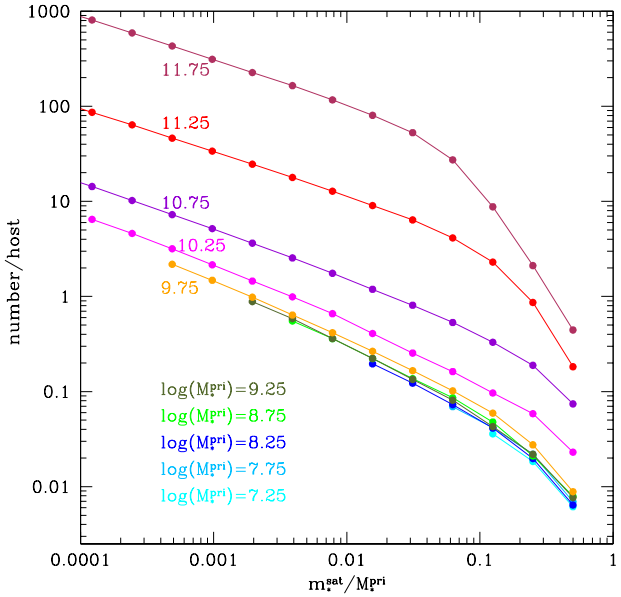

Figure 2. Cumulative number of satellite galaxies within the virial radius of primaries in the semi-analytic model of galaxy formation from Guo et al. (2011a). Symbols of different colors indicate the average number of satellites computed after binning primaries by mass in 0.5 dex-width bins of $M_{\rm pri}$. Note that, on average, the number of satellites decreases with decreasing primary mass down to $M_{\rm pri} \sim 10^{10}\,M_\odot$. Below this mass the scaled satellite mass function becomes independent of primary mass.

Interestingly, this trend does not hold for lower primary masses. The satellite abundance, expressed in terms of $m_*^{\rm sat}/M_*^{\rm pri}$, becomes *independent of primary mass* in the dwarf-galaxy regime ($M_*^{\rm pri} < 10^{10} M_\odot$). As discussed in Sec. 1, this reflects the featureless power-law scaling between galaxy and halo masses in these scales and is a prime prediction of the model testable by observation.

In order to take into account how projection effects and the presence of interlopers may affect this result, we repeat the analysis using only projected positions and line-of-sight velocities, as described in Sec. 2.2. This enables us to select primaries and satellites in identical ways for both model and observational datasets.

Fig. 3 shows, for the mock (left) and SDSS (right) samples, the average number of satellites with r-band magnitude difference equal to or smaller than $\Delta M = M_r^{\rm pri} - M_r^{\rm sat}$. (This is the simplest observational analog of the stellar mass ratio.) As in Fig. 2, we bin primaries according to their stellar mass, as indicated in the legends. Error bars correspond to 100 bootstrap resamplings of the data.

The left panel in Fig. 3 shows that the projected data behave similarly to the 3D sample: the abundance of satellites at given ΔM increases with $M_*^{\rm pri}$ for bright primaries (Guo et al. 2011b; Wang & White 2012) but becomes independent of mass for dwarf primaries ($M_*^{\rm pri} < 10^{10} M_\odot$). The overall behaviour is in strikingly good agreement with the SDSS satellite abundances, shown on the right. Despite the large error bars in the faint-primary bins (an unavoidable consequence of the limited effective volume sur-

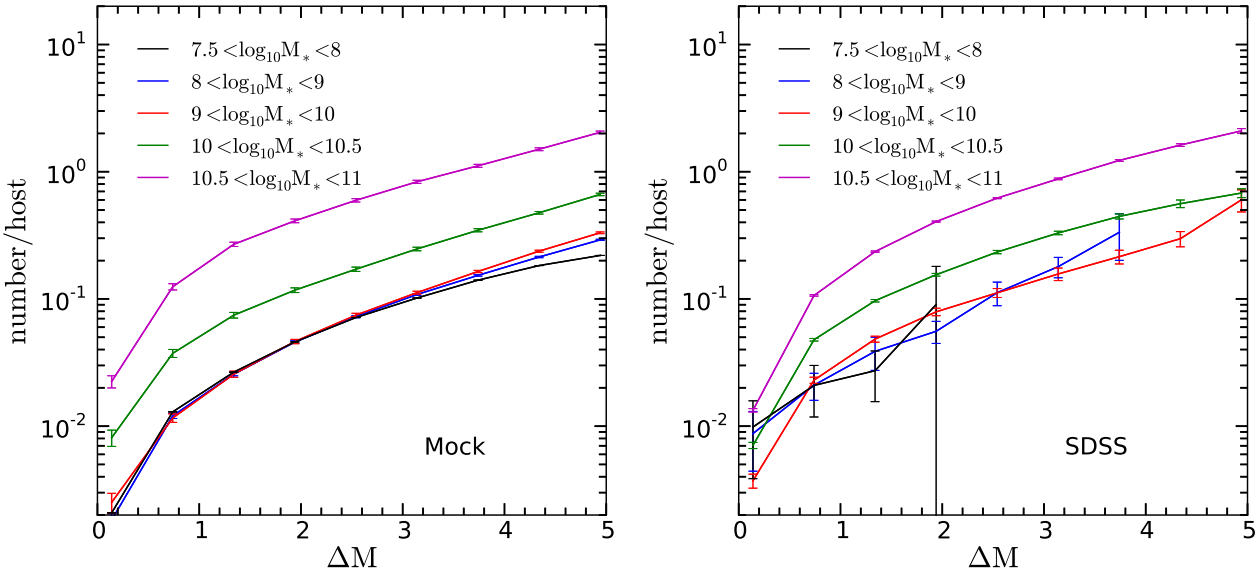

Figure 3. Average number of satellites per primary with a r-band magnitude difference smaller or equal to $\Delta M = M_r^{\rm sat} - M_r^{\rm pri}$. Each curve correspond to a given primary stellar mass range, as indicated by the labels. The left panel is for mock data from the semi-analytic catalogue. Primary/satellite galaxies are identified in projection, as outlined in Sec 2.1. Error bars show uncertainties from 100 bootstrap resamplings. Note the lack of dependence on $M_*^{\rm pri}$ for $M_*^{\rm pri} < 10^{10} M_\odot$. *Right:* Same but for galaxies in the SDSS/DR7 spectroscopic catalogue. As in the left panel, isolated dwarfs with stellar mass $7.5 < \log(\mathrm{M}_*^{\rm pri}/\mathrm{M}_\odot) < 10$ seem to populate similar dark matter haloes, $M_{200} \sim 10^{10} - 10^{11} M_\odot$ according to the simulations.

veyed by SDSS) the observed trends in satellite count with primary stellar mass closely resemble those in the mock catalogue. We interpret this result as providing strong evidence in support of the nearly power-law dependence of galaxy mass on halo mass on dwarf galaxy scales advocated by semianalytic models of galaxy formation in the ΛCDM scenario.

One concern regarding this interpretation arises from the completeness of SDSS spectroscopic data on dwarf galaxy scales. The sample is, on average, 90% complete at our apparent magnitude limit of $m_r = 17.7$. We partially correct for biases by weighting satellites and primaries with their FGOTMAIN value, which characterizes the completeness of SDSS in a given region of the sky due to fiber collision (Blanton et al. 2005). However, the completeness might worsen if objects of low surface brightness, such as many dwarfs, are systematically missed. The results in Fig 3 would then represent lower-limits to the true satellite abundance, but would still provide useful constraints on the halo mass of their hosts. We notice, however, that if our results were strongly affected by low-surface brightness biases, the good agreement between observations and the semianalytic model would be puzzling. Nevertheless, this point requires further validation once surveys with improved surface brightness sensitivity become available.

In addition to providing hints about the power-law nature of the M_*-M_{200} relation at the low-mass end, satellite number counts can also help constrain its slope. Assuming that satellite and primary galaxies follow the same $M_* \propto M_{200}^\beta$ power-law relation and that the substructure mass function is self similar, as predicted by CDM[2], then the abundance of faint satellites should scale roughly with $N(>\mu_*) \propto \mu_*^{(\alpha/\beta)}$, where $\mu_* = m_*^{\rm sat}/M_*^{\rm pri}$. Notice that this behaviour is only expected over the mass ranges where the substructure mass function is a power law, which typically requires $\mu \leqslant 0.1$ (e.g. Gao et al. 2004). This imposes an upper limit $\mu_* = 0.1^\beta \sim 0.003$ on the relative mass of the companions where we expect $N(>\mu_*) \propto \mu_*^{(\alpha/\beta)}$ to hold.

In the semianalytic model, $\alpha/\beta \sim 1.25/2.4 \sim 0.5$ (Wang et al. 2012; Guo et al. 2011a), which is in good agreement with the slope of the satellite mass function in Fig. 2 measured for low-mass companions $m *^{\rm sat}/M_*^{\rm pri} \leqslant 0.003$. This relation is independent of $M_*^{\rm pri}$, provided the simulation resolves satellites differing by three or more orders of magnitude in stellar mass with respect to $M_*^{\rm pri}$. This, in our simulations, happens at $M_*^{\rm pri} \geqslant 10^{10} M_\odot$. Interestingly, the scatter in stellar mass at fixed halo mass, which in the model is ~ 0.35 dex for the low-mass objects (Guo et al. 2011a), does not seem to impact the slope derived from the simple arguments given previously. However, this would change if the scatter in the M_*-M_{200} relation were strongly correlated to the halo mass. In our case this correlation is rather mild.

We conclude from Fig. 3 that the good agreement in shape, normalization and slope between SDSS primaries and the mock catalogue strongly favours a power-law relation with a steep slope $M_* \propto M_{200}^{2.5}$ between stellar mass and halo mass of dwarf galaxies. This agrees with predictions from the semianalytic model of Guo et al. (2011a) and from extrapolations of abundance-matching studies (e.g., Moster et al. 2010; Behroozi et al. 2010; Guo et al. 2010).

4 SUMMARY

We study the abundance of satellites as a function of primary stellar mass in the Sloan Digital Sky Survey. Using the SDSS/DR7 spectroscopic sample from the NYU-VAGC catalogue we are able to

[2] $N(>\mu) \propto \mu^\alpha$ for small μ, where $\mu = m_{\rm DM}^{\rm sub}/M_{\rm DM}^{\rm host}$ is the ratio of the dark matter masses of subhalo and host and $\alpha \sim -1$ (Gao et al. 2004)

extend previous studies to significantly fainter primaries, $M_*^{\rm pri} = [10^{7.5}\text{-}10^{11}]M_\odot$. In agreement with previous work, we find that the abundance of satellites exceeding a given satellite-to-primary stellar mass ratio, $m_*^{\rm sat}/M_*^{\rm pri}$, depends strongly on $M_*^{\rm pri}$ for bright primaries. On the other hand, *the abundance of satellites around dwarf primaries, $M_*^{\rm pri} < 10^{10}M_\odot$, is approximately independent of primary stellar mass*.

These results are in excellent agreement with predictions of semi-analytic models within ΛCDM. These trends arise from the mass invariance of substructure in CDM haloes and from the varying efficiency of galaxy formation as a function of halo mass. On dwarf galaxy scales, where the relation between galaxy mass and halo mass is well approximated by a steep power law, the invariance of satellite abundance with primary mass reflects directly the scale-free nature of substructure. Around bright galaxies the scaling between galaxy mass and halo mass deviates from a simple power law, leading to the observed strong increase of satellite abundance with increasing primary mass.

The good agreement in shape and normalization between satellite counts in SDSS and those in the mock catalogue provides support for a steep stellar-halo mass relation for dwarfs, consistent with the $M_* \propto M_{200}^{2.5}$ predicted both by semi-analytic models and by extrapolations of current abundance-matching analyses. More definitive constraints on the slope of the M_*-M_{200} relation for dwarf galaxies may come from a robust determination of the slope of satellite abundances around isolated primaries in tandem with studies of the effect of scatter in the stellar mass - halo mass relation. Probing increasingly fainter companions in observational surveys of the surroundings of isolated dwarfs may prove crucial for this goal.

ACKNOWLEDGEMENTS

LVS is grateful for financial support from the CosmoComp/Marie Curie network. The authors thank the hospitality of the Kavli Institute for Theoretical Physics, Santa Barbara, where part of this work was completed. This research was supported in part by the National Science Foundation under Grant No. NSF PHY11-25915.

REFERENCES

Abazajian K. N., Adelman-McCarthy J. K., Agüeros M. A., Allam S. S., Allende Prieto C., An D., Anderson K. S. J., Anderson S. F., Annis J., Bahcall N. A., et al. 2009, ApJS, 182, 543

Behroozi P. S., Conroy C., Wechsler R. H., 2010, ApJ, 717, 379

Blanton M. R., Schlegel D. J., Strauss M. A., Brinkmann J., Finkbeiner D., Fukugita M., Gunn J. E., Hogg D. W., Ivezić Ž., Knapp G. R., Lupton R. H., Munn J. A., Schneider D. P., Tegmark M., Zehavi I., 2005, AJ, 129, 2562

Boylan-Kolchin M., Besla G., Hernquist L., 2011, MNRAS, 414, 1560

Boylan-Kolchin M., Bullock J. S., Kaplinghat M., 2012, MNRAS, 422, 1203

Brainerd T. G., 2005, ApJL, 628, L101

Conroy C., Prada F., Newman J. A., Croton D., Coil A. L., Conselice C. J., Cooper M. C., Davis M., Faber S. M., Gerke B. F., Guhathakurta P., Klypin A., Koo D. C., Yan R., 2007, ApJ, 654, 153

Erickson L. K., Gottesman S. T., Hunter Jr. J. H., 1999, ApJ, 515, 153

Ferrero I., Abadi M. G., Navarro J. F., Sales L. V., Gurovich S., 2011, ArXiv 1111.6609

Gao L., White S. D. M., Jenkins A., Stoehr F., Springel V., 2004, MNRAS, 355, 819

Guo Q., Cole S., Eke V., Frenk C., 2011a, ArXiv 1101.2674

Guo Q., Cole S., Eke V., Frenk C., 2011b, MNRAS, 417, 370

Guo Q., White S., Li C., Boylan-Kolchin M., 2010, MNRAS, 404, 1111

Kravtsov A. V., Berlind A. A., Wechsler R. H., Klypin A. A., Gottlöber S., Allgood B., Primack J. R., 2004, ApJ, 609, 35

Lares M., Lambas D. G., Domínguez M. J., 2011, AJ, 142, 13

Lorrimer S. J., Frenk C. S., Smith R. M., White S. D. M., Zaritsky D., 1994, MNRAS, 269, 696

McKay T. A., Sheldon E. S., Johnston D., Grebel E. K., Prada F., Rix H.-W., Bahcall N. A., Brinkmann J., Csabai I., Fukugita M., Lamb D. Q., York D. G., 2002, ApJL, 571, L85

Moore B., Ghigna S., Governato F., Lake G., Quinn T., Stadel J., Tozzi P., 1999, ApJL, 524, L19

Moster B. P., Somerville R. S., Maulbetsch C., van den Bosch F. C., Macciò A. V., Naab T., Oser L., 2010, ApJ, 710, 903

Nierenberg A. M., Auger M. W., Treu T., Marshall P. J., Fassnacht C. D., 2011, ApJ, 731, 44

Papastergis E., Martin A. M., Giovanelli R., Haynes M. P., 2011, ApJ, 739, 38

Prada F., Vitvitska M., Klypin A., Holtzman J. A., Schlegel D. J., Grebel E. K., Rix H.-W., Brinkmann J., McKay T. A., Csabai I., 2003, ApJ, 598, 260

Springel V., Yoshida N., White S. D. M., 2001, New Astronomy, 6, 79

Tully R. B., Rizzi L., Dolphin A. E., Karachentsev I. D., Karachentseva V. E., Makarov D. I., Makarova L., Sakai S., Shaya E. J., 2006, AJ, 132, 729

van den Bosch F. C., Norberg P., Mo H. J., Yang X., 2004, MNRAS, 352, 1302

Wang J., Frenk C. S., Navarro J. F., Gao L., Sawala T., 2012, MNRAS, p. 3369

Wang W., White S. D. M., 2012, MNRAS, p. 3394

Zaritsky D., Smith R., Frenk C., White S. D. M., 1997, ApJ, 478, 39

Zwaan M. A., Meyer M. J., Staveley-Smith L., 2010, MNRAS, 403, 1969